

## The External Kink Mode and the Role of $q_{95}$ in Diverted Tokamaks

A.D. Turnbull<sup>1</sup>, J.M. Hanson<sup>2</sup>, F. Turco<sup>2</sup>, N.M. Ferraro<sup>3</sup>, M.J. Lanctot<sup>1</sup>, L.L. Lao<sup>1</sup>, E.J. Strait<sup>1</sup>, P. Piovesan<sup>4</sup>, and P. Martin<sup>4</sup>

<sup>1</sup>General Atomics, San Diego, California USA

<sup>2</sup>Columbia University, New York, New York, USA

<sup>3</sup>PPPL, Princeton, New Jersey, USA

<sup>4</sup>Consorzio RFX, Padova, Italy

### Abstract

The disruptive instability in diverted tokamaks when  $q$  at the 95% poloidal flux surface,  $q_{95}$ , is driven below 2.0 is shown to be a resistive kink. The mode is a resistive counterpart to the current driven ideal mode that traditionally explained the disruption in limited cross sections when  $q_a$ , the safety factor at the outermost closed flux surface, lies just below a rational value. Diverted plasmas, in which  $q_a$  is formally infinite in the MHD model, have presented a longstanding difficulty since the theory would predict stability, yet, the disruptive limit occurs in practice when  $q_{95}$  reaches 2. Numerical calculations show the resistive kink mode is linearly destabilized by the rapidly increasing resistivity at the plasma edge when  $q_{95} < 2$ , but  $q_a \gg 2$ . The resistive kink also occurs for limiter plasmas but quickly transforms to the ideal mode when the rational surface exits the plasma; this also explains an observed small discrepancy in onset conditions.

### I Introduction

The disruptions observed in tokamaks during the current ramp as the edge safety factor  $q_a$  passed through rational values were well explained as ideal magnetohydrodynamic (MHD) external kink modes. In particular,  $q_a = 2$  appears to be a hard experimental and theoretical limit. However, with the advent of diverted boundary plasmas, the theory naively predicts complete stability to these modes since  $q_a$  is formally infinite. Nevertheless, disruption events continued to be observed in diverted discharges when  $q$  at the 95% flux surface,  $q_{95}$ , passed through rational values. Ideal theory could only explain this by assuming the real edge of the plasma to be the 95% surface. Recent tokamak experiments in RFX-mod and DIII-D, which explored the  $m/n = 2/1$  mode at  $q_a \sim 2$  and  $q_{95} \sim 2$  [1], brought the issue to a head since no meaningful stability analysis was possible for the divertor case. The present paper resolves the issue by invoking a realistic resistivity profile rising to large vacuum-like values in the very edge. Several models for the profile are considered, all

yielding qualitatively similar results. A resistive kink is found to be unstable with large growth rate,  $\gamma$ , but with  $\gamma$  depending on resistivity.

## II External Resistive Kink in Diverted and Limited Discharges

The experiments in DIII-D L-mode limiter and diverted cross sections are described in Refs [1]. Ideal MHD stability calculations using reconstructed equilibria from two representative discharges at mode onset found stability in both configurations, consistent with the reconstructed edge  $q$  just above 2.0 ( $q_a = 2.08$ ) in the limiter case and well above 2.0 in the diverted case; while formally infinite, the edge  $q$  in that case is typically numerically in the range 3 to 6.

With a small cut off of the edge to yield an equilibrium with  $q_a = 1.99$ , the limiter case was found to be unstable to a fast growing ideal 2/1 kink mode, consistent with the theory. The predicted ideal instability is also consistent with the observed magnetic fluctuation signals [1]. However, the cutoff procedure applied to the diverted case continued to yield ideal stability. All attempts at reconstructing the diverted equilibrium found ideal stability except for special cases where the cutoff yielded  $q_a$  in a narrow band just below an integer, consistent with the theory, but that cannot readily explain the disruption.

In ideal MHD stability theory, stability to current driven external kinks is determined by whether the respective rational surface falls in the infinitely conductive or infinitely resistive region. An alternative to a cutoff of the edge is to invoke a realistic resistivity profile, effectively smoothing the transition. Several different alternative profiles were considered, namely the Spitzer profile,  $\eta \sim \eta_0 T_e^{-3/2}$ , the Sauter model [2], which includes neoclassical corrections, and an effective profile calculated from Ohms Law and time dependent equilibrium reconstructions to obtain the current density and the parallel electric field. In addition, an enhancement provided by a Gaussian multiplicative form factor of amplitude  $A$  and width  $w$  was incorporated in each of the models to enable control of the profile near  $q = 2$ . The profiles are shown in Figure 1, including an example with the enhancement applied. Details are given in [3].

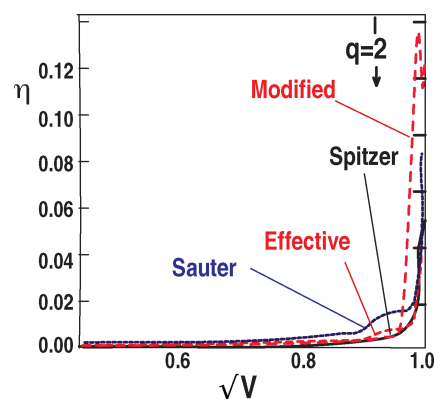


Fig. 1. Model resistivity profiles showing the Spitzer (solid), Sauter (long dash), and effective (short dash) profiles. Also shown is the effective profile with additional enhancement near  $q = 2$  (dotted).

Stability calculations using the MARS code found that for  $\eta_{q=2} \equiv \eta(q=2)$  sufficiently large, a resistive kink is unstable with ideal level growth rates. Small enhancements were typically sufficient for the Sauter and effective profiles to yield a well-resolved instability.

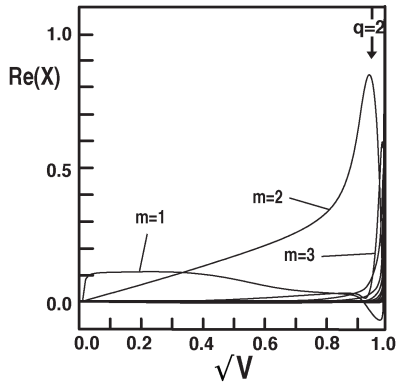


Fig. 2. Resistive kink eigenmode computed using MARS for the diverted DIII-D discharge #150513 showing the Fourier decomposition of the normal displacement  $X \equiv \xi \cdot \nabla \Psi$  with respect to the straight field line angle as a function of normalized volume.

Large enhancements, typically used for the Spitzer case, tended to shift the steep region inward slightly. Figure 2 shows an example using the effective resistivity profile with a small enhancement. This assumed a real resistive wall at the location of the DIII-D conducting wall. The mode is an external, predominantly mixed 2/1 and 3/1 with kink parity, with a growth rate normalized to a toroidal Alfvén time of

$$\gamma \tau_A = 0.08 \text{ and a small real frequency of}$$

$$\omega \tau_A = -0.4 \times 10^{-2} \text{ arising from both the resistive plasma and the resistive wall.}$$

For the limiter discharge,  $q_a$  is strongly constrained by the well diagnosed total current and cross

section shape, and the disruption onset appeared when  $q_a = 2.08 \pm 0.01$ , estimated from a Monte-Carlo analysis [1]. This slight discrepancy is resolved by a similar resistive stability analysis and a resistive kink is then found to be already unstable with  $q_a = 2.08$ . The mode structure is qualitatively similar to the ideal mode found with  $q_a < 2$  [1,3].

Synthetic diagnostic predictions of the magnetic fluctuation signals using the resistive kink modes in both discharges are in good agreement with the experimental diagnostic data [3]. For the limiter case the agreement is similar to the ideal comparison in Ref 1. However, the resistive kink explanation does not require a modification (i.e. a cutoff) of the equilibrium to obtain this agreement. For the diverted discharge, the agreement is similarly excellent [3].

### III Resistive Kink Scaling

Scaling studies from a large number of sensitivity studies with varying resistivity profile types, normalization factors, and enhancement factors were performed. While the growth rates are ideal-like, they do depend on resistivity and are particularly sensitive to the value near the  $q=2$  surface. The aggregate growth rates are shown in Figure 3 for the two discharge types as a function of  $\eta_{q=2}$ . In both, over the experimentally relevant midrange of resistivity values, the scaling conforms to  $\gamma \sim \eta^\nu$  with  $\nu \approx 1/3$ , characteristic of a resistive kink [4].

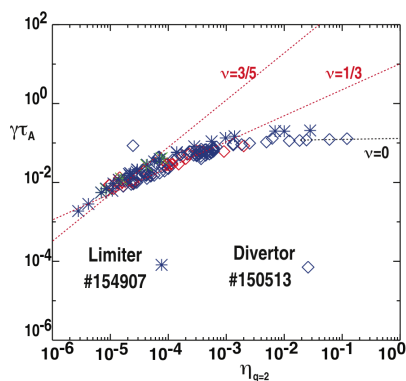


Fig. 3. Scaling of aggregated resistive kink mode growth rates overlaid for discharges #150513 and #154907 with

$\eta_{q=2}$ . The lines indicate the varying local scalings.

Nonetheless, it is clear that the exponent varies continuously over a range  $0 \leq \nu \leq 1$  and the scaling is best characterized as  $\gamma \sim \eta^{\nu(\eta)}$ , where  $0 \leq \nu(\eta) \leq 1$  is a slowly varying and monotonically decreasing function of  $\eta_{q=2}$ . The transitions in  $\nu$  are smooth and do not coincide with any mode structure change. This is in contrast to previous studies that typically found distinct transitions from tearing parity when  $\nu \cong 3/5$  to kink parity when  $\nu \cong 1/3$  [4]. In the present case, the kink parity is completely dominant for the  $m = 2$  component (some parity mixing does occur at finite  $\beta$ ). The crucial difference appears to be related to the constant resistivity profile used in most of the earlier studies. In Figure 3, the scaling in both discharges also asymptotes smoothly to the ideal scaling limit with  $\nu = 0$  at the highest  $\eta_{q=2}$  values, making clear the connection between the ideal model.

#### IV Summary and Conclusion

The resistive kink provides a convincing explanation for the observed kink-like modes in L-mode diverted discharges that lead to the disruptive events during tokamak current ramps. While the usual ideal theory works well for limiter cross sections, it completely fails to predict the instability in the diverted case. The resistive kink model also explains puzzling details in the limiter case as well. In both, synthetic diagnostic predictions of the magnetic fluctuations agree well with the measured signals. From a large number of studies of the sensitivity of the results to the profile, the growth rate was found to scale with a power law of the form  $\gamma \sim \eta^\nu$ , but with  $\nu$  a weak function of  $\eta_{q=2}$  varying continuously over  $0 \leq \nu \leq 1$ , with no distinct transitions in mode structure, and continuing up to the ideal scaling  $\nu \cong 0$ . Future work is intended to consider the instability in diverted H-mode plasmas.

#### Acknowledgements

Work support by the U.S. DOE under DE-FC02-04ER54698<sup>1</sup> and DE-FG02-95ER54309<sup>1</sup>, DE-FG02-04ER54761<sup>2</sup> and DE-AC02-09CH11466<sup>3</sup>.

#### References

- [1] Hanson J.M., *et al.*, 2014 *Phys. Plasmas* **21**, 072107
- [2] Sauter O., *et al.*, 1999 *Phys. Plasmas* **6**, 2834
- [3] Turnbull A.D. *et al.*, 2016 *J Plasma Phys.* Shafranov Memorial edition
- [4] Huysmans G.T.A., *et al.*, 1993 *Phys. Plasmas* **B5**, 1545